Colloid Polym Sci (2006) 284: 1163–1169
DOI 10.1007/s00396-006-1498-3

ORIGINAL CONTRIBUTION

Tapasi Kotoky
S. K Dolui

Synthesis of polystyrene/silica hybrid composites by the sol–gel method: effect of introduction of a flexible component (butyl acrylate) into the silylated polystyrene backbone

Received: 27 December 2005
Accepted: 31 March 2006
Published online: 23 May 2006

T. Kotoky · S. K. Dolui (✉)
Department of Chemical Sciences,
Tezpur University,
Napaam, Assam 784028, India
e-mail: dolui@tezu.ernet.in

Abstract Polystyrene/silica, polystyrene–butylacrylate/silica, silylated polystyrene/silica, and silylated polystyrene–butylacrylate/silica hybrid composites were synthesized by the sol–gel method in tetrahydrofuran using HCl as catalyst and tetraethylorthosilicate as the silica precursor. The polymers were characterized by fourier transform infrared (FTIR), nuclear magnetic resonance, and gel permeation chromatography. The sol–gel mixtures were cast on glass plates and dried in air at 30°C for 72 h. The composites were characterized by FTIR, thermogravimetric analysis, differential scanning calorimetry, and scanning electron microscopy analysis. Silica (12.8%) could be incorporated within the silylated polystyrene–butylacrylate matrix while retaining optical transparency. These composites showed better thermal stability and water resistance in comparison to the individual polymers.

Keywords Hybrid composites · Sol–gel method · Scanning electron microscopy (SEM) · Optical transparency · Thermal properties

Introduction

The sol–gel method, a homogeneous room temperature solution method, has emerged as a versatile tool for the synthesis of hybrid composites from organic and inorganic components. The method allows the control of bulk properties of materials by controlling the composition and microstructure at the molecular level [1–10]. Most importantly, it enables the synthesis of optically transparent materials because the organic and inorganic domains in the hybrid remain well below the wavelength of visible light. Briefly, the sol–gel method involves the hydrolysis of a metal oxide or alkoxide precursor solution to form a colloidal dispersion known as "sol", which then undergoes crosslinking to form a three dimensional crosslinked network known as "gel" [11].

The major problem encountered with hybrid synthesis is maintaining the homogeneity of the sol–gel mixture. Homogeneity in the organic–inorganic sol–gel mixture is affected by various factors such as pH, solvent, water to alkoxide ratio, concentration, catalyst, and temperature [12–16]. Each of these factors plays an important role in the gelation process and the structure of the final products. The effect of the above parameters was earlier reported by us for two hybrid systems, poly (vinylalcohol)/silica [17], and silylated polystyrene/silica [18]. It was observed that the generation of a stable colloidal system helped to attain better properties in the composite materials and the silylation of the polymer backbone enhances compatibility with the silica phase.

For hybrid synthesis within a polystyrene matrix, the brittleness of polystyrene causes phase separation between polymer and silica particles. Therefore, it was not possible to incorporate a higher amount of silica within the polymer matrices.

The brittleness of polystyrene may be reduced by the incorporation of a flexible component such as butyl acrylate. In this work, we have attempted to study the effect of incorporating butyl acrylate on the properties of hybrid composites synthesized through the sol–gel method.

Experimental

Raw materials

Tetraethylorthosilicate (TEOS) (Merck–Schuchardt), methylvinyldichlorosilane (Fluka), benzoyl peroxide (SD Fine Chem), and butyl acrylate (SD Fine Chem) were used as received. Styrene (Merck–Schuchardt) was purified by removing inhibitor with sodium hydroxide solution followed by drying over molecular sieves.

Synthesis of polystyrene, silane functionalized copolymers of styrene and methyl vinyl dichlorosilane (PS/MVS) and silane functionalized copolymers of styrene, butyl acrylate, and methyl vinyl dichlorosilane (PS/BA/MVS).

Polystyrene was synthesized by the solution method following a standard procedure [18]. Copolymers were synthesized from styrene, butylacrylate (BA), and methylvinyldichlorosilane (MVS), using the concentrations listed in Table 1. The copolymers were synthesized by changing the proportion of monomers. A typical method for the synthesis of copolymers PS/MVS is given.

Fifteen milliliter of styrene and 40 ml of benzene were taken together in a three-necked flask fitted with a condenser, a mechanical stirrer, and a nitrogen inlet. Then, 0.5 ml of methylvinyldichlorosilane (MVS) was added drop-wise with constant stirring. The temperature was raised to 70°C and 0.15 g of the initiator benzoyl peroxide was added. The polymerization was continued at a temperature of 70°C over a period of 3 h. The copolymer (PS/MVS) was precipitated in cold ethanol and purified by dissolving in tetrahydrofuran (THF) and reprecipitation in ethanol. The composition of the reaction mixture was varied by changing the ratio of styrene, methylvinyldichlorosilane, and butyl acrylate (BA) as discussed below.

The polymerization yield was ~95% and Mn (g/mole) was higher than 35,000 in all cases. The repeat units of the copolymers are shown below in Fig. 1. Inherent viscosities were around 0.5 dl/g. The viscosity of a 0.5% solution in THF was measured using Ubbelohde viscometer at 30°C and reported in terms of inherent viscosity $[\eta]=[(\ln t/t_0)/c]$. Where "t_o" is the time taken by the solvent THF and "t" is the time taken by the solution and "c" is the concentration of the polymer solution which is expressed in units of grams/deciliter (g/dl). The inherent viscosity, which is inversely proportional to the concentration, is therefore expressed in units of dl/g.

Table 1 Molar composition of copolymers

SL	Sample	Styrene (mol)	Butylacrylate (mol)	MVS (mol)
1	PS	0	0	0
2	PS/MVS (1)	0.129	0	0.0025
3	PS/MVS (2)	0.129	0	0.005
4	PS/MVS (3)	0.129	0	0.100
5	PS/BA	0.095	0.042	0
6	PS/BA/MVS (1)	0.095	0.042	0.006
7	PS/BA/MVS (2)	0.095	0.042	0.125

Preparation of colloidally stable sol from tetraethyl orthosilicate (TEOS) solution

Sol–gel mixtures were prepared using TEOS, HCl (1 N) and tetrahydrofuran(THF). 1 N HCl was added with constant stirring at 60°C to the TEOS solution in THF. Addition of acid catalyst was stopped just before the point of gelation, which was taken to be the point at which the mixture became viscous. The amount of acid catalyst necessary for the preparation of colloidally stable sol required was noted.

Preparation of sol–gel mixtures from TEOS in presence of solution of copolymer and composite films thereof

TEOS solution was added with stirring to the solution of copolymer in solvent (toluene in case of polymers PS/MVS and THF in case of polymers PS/BA/MVS[1]) to form a homogeneous mixture. Then the acid catalyst (1 N HCl) (the amount of which was determined from the previous experiment), was added slowly with stirring at a temperature of 60°C. The solution was stirred at 60°C for 30 min to carry out the in-situ acid hydrolysis of TEOS within copolymer solution. The sol–gel mixtures were then poured over glass plates to give composite films. The films on glass plates were then dried in air at 30°C over a period of 72 h and finally dried in the oven at 60°C for 5 h. These composite films were analyzed by Fourier transform infrared (FTIR), scanning electron microscopy (SEM), and thermogravimetric analysis (TGA).

Characterization

FTIR The dried composite films cast over glass plate were used for spectroscopic analysis. The IR spectra were recorded in a FTIR spectrophotometer (Nicolet USA, Impact 401).

SEM analysis The samples for scanning electron microscopy were prepared in the form of thin film on glass plates. The samples were kept in desiccators for 2 h and then coated with gold. The tests were conducted by using a scanning electron microscope (Jeol, Japan). The magnification and acceleration voltages varied from 20 kV×150 to 20 kV×1,000.

[1] THF, which is an irritant that could be avoided in the first case but was used in the second case as it is a better cosolvent for the mixture.

Fig. 1 Repeat unit of copolymers

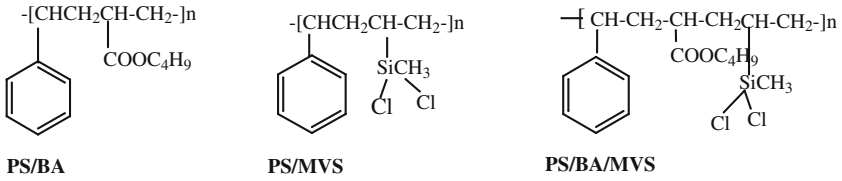

NMR analysis ^{1}HNMR analysis was carried out with a 400 MHz Brucker nuclear magnetic resonance (NMR) spectrometer using $CDCl_3$ as solvent.

GPC analysis Gel permeation chromatography (GPC) analysis for the copolymers were carried out using GPC (Water, USA, Model 515) solvent delivery system at a flow rate of 1 ml/min through a set of three ultrastyregel columns. Analysis was done at controlled temperature at 45°C using high performance liquid chromatography (HPLC) grade tetrahydrofuran (THF) as eluent using polystyrene as standard.

TGA analysis TGA analysis for the copolymer and composites were carried out with a PYRIS1 thermogravimetric analyzer (Shelton, USA) in nitrogen atmosphere at a heating rate of 10°C/min within a temperature range of 50 to 700°C.

Water uptake experiment The relative rate of water absorption under saturated conditions was measured by initially drying the films in a vacuum oven at 50°C for 12 h, immersing the films in distilled water, and then measuring the weight change until it became constant. Water absorption by the films under saturated conditions was measured following the procedure in ASTM-D570-81.

Structure analysis of copolymers The NMR and FTIR spectral data for copolymers are discussed below:

PS/MVS

^{1}H NMR $CDCl_3$ (δ, ppm): 7.4, 7.48, 7.41, 7.34, 7.25, and 7.1 (aromatic protons) 6.59, 1.45, 1.86, and 1.27 due to the four different proton environments.

PS/BA

^{1}H NMR $CDCl_3$ (δ, ppm): 3.75 (alkyl protons attached to $COOC_4H_9$); 2.7 (–CH attached to –$COOC_4H_9$); and 1.2–1.8 (alkane protons)

PS/BA:

^{13}C dimethylsulfoxide (DMSO) d_6 (δ, ppm): 13, 19, 30, 41, and 63 (alkane C incorporated from the butyl group). 126, 127, 128,143, and 145 due to aromatic protons.

PS/BA/MVS:

^{1}H NMR $CDCl_3$ (δ, ppm): 7.1–6.64 (aromatic protons); 4.17 is due to butyl group attached to COO; 2.7 due to CH attached to $COOC_4H_9$; and 1.2 to 1.8 (alkane protons).

FTIR

The bands due to polystyrene are as follows: 1,490 cm^{-1} (alkene CH_2 bending); 765 cm^{-1} (aromatic CH bending); 2,929 cm^{-1} aromatic CH stretching) 1,594 cm^{-1} (aromatic C–C multiple bond stretch); 753 cm^{-1} (aromatic C–H stretch) [19].

PS/MVS

In addition to the above bands, due to the polystyrene moiety, the copolymer PS/MVS shows bands at 1,267 cm^{-1} (CH_3 symmetric deformation of Si–CH_3 group); 3,027 cm^{-1}, (alkene C–H stretch due to monosubstituted vinyl group); 2851 cm^{-1} (alkane C–H stretch); 906 cm^{-1} (alkene C–H bending due to monosubstituted vinyl group); 538 cm^{-1} and 440 cm^{-1} (Si–Cl stretching vibration).

PS/BA/MVS

In addition to the bands due to the PS/MVS moiety, a band at 723 cm^{-1} (COO-stretching vibration) is observed.

FTIR spectral data for silica and composites

Silica: 1,037, 1,085, and 1,166 cm^{-1} (broad split band due to Si–O–Si).

(PS/MVS)/silica: 1,070–1,150 cm^{-1} (Si–O–Si linkages); 1,267 cm^{-1} (CH_3 symmetric deformation of Si–CH_3 group) (in addition to the bands due to polystyrene group).

(PS/BA/MVS)/silica: 1,070–1,150 cm^{-1} (Si–O–Si linkages); 1,723 cm^{-1} (COO-stretching vibration) (in addition to the bands due to PS/MVS group).

The presence of the Si–O–Si bands in the composites is noteworthy, and points to the formation of linkages with the polymeric moiety.

Results and discussion

Preparation of colloidally stable sol from TEOS solution and in situ acid hydrolysis of TEOS in the copolymer matrices

The scheme in Fig. 2 shows the sol–gel reaction and composite formation of copolymers with silica. The mole ratios of polymer: TEOS to HCl to THF to H_2O used for the sol–gel synthesis are given in Table 2. The amount of acid catalyst (1 N HCl) required to form the sol decreased with an increase in the concentration of TEOS. The reason may be attributed to the fact that aggregation of silica particles

to form sol increases with an increase in the silica concentration. As the silane content in the copolymers increased, the amount of TEOS in the mixture could be increased. Silylation enhances compatibility between phases. This is because in the absence of the silylating monomer, gel formation proceeds only through condensation of Si–OH of TEOS. In the presence of a silylating monomer, gel formation proceeds through two ways:

1. Condensation of Si–OH of TEOS.
2. Condensation of Si–OH of TEOS and Si–OH of polymer.

This helps to compatibilize the silica phase within the silylated polymer phase [18]. In sol-formation, the first step is the hydrolysis of TEOS and the second stage is the condensation forming Si–O–Si linkages. In gelation stage, extended networks of Si–O–Si form.

Morphology The optical transparency can be used as an initial criterion for judging the formation of a homogeneous phase of both inorganic and organic constituents. When macroscopic phase separation occurs, products look opaque because the large domain size in the inorganic oxide causes light scattering in the system [20]. The composition, appearance, and morphological characteristics of the composite materials are listed in Table 2 for the copolymers and their composites. The SEM micrograph for polystyrene/silica composite (Fig. 3a; accelerating voltage 20 kV×150) shows that phases are separated. The silylated polystyrene/silica composites are optically transparent and do not show any distinct phase separation

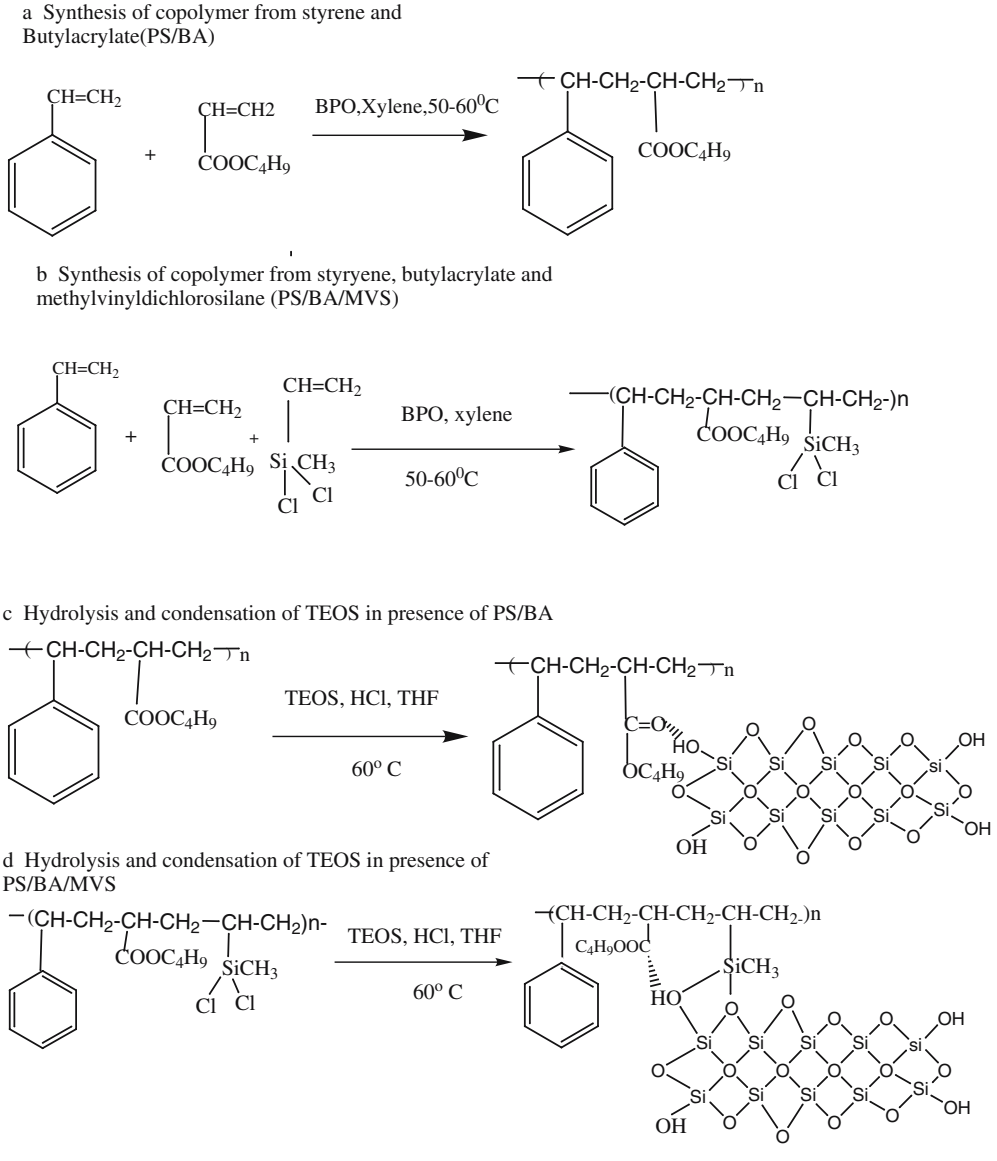

Fig. 2 Synthesis of copolymers PS/BA and PS/BA/MVS and hydrolysis and condensation of TEOS in presence of copolymers PS/BA and PS/BA/MVS. The structure for bonding interactions between the –CO group of polymer and –OH groups of hydrolyzed silanol is only one of the possible modes envisaged and by no means conclusive

Table 2 Composition of sol–gel mixtures, morphology, thermal, and water uptake properties of the copolymers and composites

SL	Sample	Mole ratio of polymer: TEOS to HCl to solvent	Appearance under SEM	Tid	Residue at 500oC	water uptake (%)
1	PS	Pure polymer	Smooth surface	150	0	0.4
2	Composite of PS and silica	0.067:0.0010;0.0014:0.0793	Phase separated	176	0.25	0.38
3	PS/MVS (1)	Pure copolymer	Smooth surface	200	0.25	0.38
4	PS/MVS (1)	Pure copolymer	Smooth surface	225	0.5	0.37
5	PS/MVS (3)	Pure copolymer	Smooth surface	225	0.8	0.35
6	Composite of PS/MVS (1)and silica	0.0288:0.0036:0.0007:0.0793	No visible phase separation	180	6	0.33
7	Composite of PS/MVS (2)and silica	0.0288:0.0036:0.0007:0.0793	Phase separation visible	220	6	0.33
8	Composite of PS/MVS (3) and silica	0.0288:0.0040:0.0002:0.0793	No visible phase separation	350	7	0.30
9	PS/BA	Pure copolymer	Smooth surface	170	0	0.45
10	Composite of PS/BA and silica	0.003:0.001:0.0002:0.123	Dispersed spherical particles	176	0.5	0.40
11	PS/BA/MVS (1)	Pure copolymer	Smooth surface	200	0.8	0.38
12	PS/BA/MVS (2)	Pure copolymer	Smooth surface	210	0.5	0.38
13	Composite of PS/BA//MVS (1) and silica	0.0002:0.0005:0.00004:0.123	Smooth surface	230	7	0.37
14	Composite of PS/BA/MVS (1) and silica	0.0002:0.0006:0.00004:0.123	Dispersed spherical particles	250	7.5	0.35
15	Composite of PS/BA/MVS (2) and silica	0.0002:0.0008:0.00005:0.123	Smooth surface	250	9	0.37
16	Composite of PS/BA/MVS (2) and silica	0.0002:0.0009:0.00005:0.123	Dispersed spherical particles	280	12.8	0.35

For PS and PS/MVS composites, the solvent is toluene; for PS/BA and PS/BA/MVS composites, the solvent is THF
T_{id} Initial degradation temperature

(Fig. 3b; accelerating voltage 20 kV×350). The polymer matrix is visible as the dark phase in the background while the silica phase appears as the bright region. Figure 3c shows the SEM micrograph for the (PS/BA)/silica composites. The physical appearance of the sample (PS/BA)/silica is transparent and the SEM micrographs do not show phase separation, but a polymer/silica interface is clearly visible (Fig. 3c; accelerating voltage 20 kV×1,000). The introduction of the butyl acrylate component enhances compatibilization with silica thereby preventing phase separation. The butyl acrylate acts as an internal plasticizer, reducing the brittleness of polystyrene. Figure 3d, e, and f show the SEM micrographs for the polymer/silica composites having PS/BA/MVS (1) and PS/BA/MVS (2) polymer matrices. On incorporating MVS, optical transparency could be retained with enhanced silica loading. The SEM micrographs in Fig. 3d,e (accelerating voltages 20 kV×1,000 and 20 kV×1,500) do not show any phase separation even at such high magnifications. Table 2 shows the silica residues at 550°C for the PS/MVS/silica composites. ~0.25 to 7% silica was loaded in the composites. For the (PS/BA/MVS)/silica composites, the silica loading is further increased to ~12.8%, while retaining optical transparency (Table 2). Figure 3f shows that spherical silica particles become visible in the PS/BA/MVS (2) matrix when the TEOS concentration is increased (accelerating voltage 20 kV×100). An explanation for this observation may be given as follows: small, stable particles are produced under low pH conditions where hydrolysis is fast and condensation is relatively slow [21]. At low pH, there are a large number of nucleation sites due to rapid hydrolysis, which depletes the solution of TEOS monomers, and small particles (2–4 nm) are formed. These species can then aggregate, via a cluster–cluster growth mechanism, to form oligomers. Polymerization is slow in this pH range, so further particle growth is almost negligible. These chains may then adopt spherical shapes, which are not densified. At higher silica percentages, the individual spheres become sufficiently large (as was observed in Fig. 3f); at lower percentages, the sizes remain below 100 A° and, therefore, not very distinctly visible [22] (SEM micrographs in Fig. 3d,e show some such spherical particles that are barely visible). According to Yoldas et al., concentrating the reaction solution results in significant polymerization if silanol groups are present [22].

TGA analysis The curves for the composite samples (curves b, c, and d in Fig. 4a,b) show higher thermal stability in comparison to the individual copolymers [(curves "a") in Fig. 4a,b).This is because of the presence of the inorganic Si–O–Si network in the composites which is absent in the copolymer. The enhancement in thermal stability of the composites could be attributed to the interaction force between silane functionalized polystyrene and silica network [23]. The initial degradation temperature (T_{id}) was obtained by second differentiation of integral TGA curves (Table 2). The TGA curves for the composites derived from PS/MVS (3) show the highest extent of thermal stability with T_{id} value reaching up to 370°C.

Water uptake The water uptake percentage for the composite samples decreases with the incorporation of silica phase as shown in Table 2. The water uptake was found to decrease on increasing the silane content in the copolymers and silica content in the composites. This is suggestive of higher hydrophobicity in the composites arising from the incorporation of a crosslinked SiO_2 network into the polymer matrix. The decrease in water uptake was the greatest for the silylated polystyrene composites.

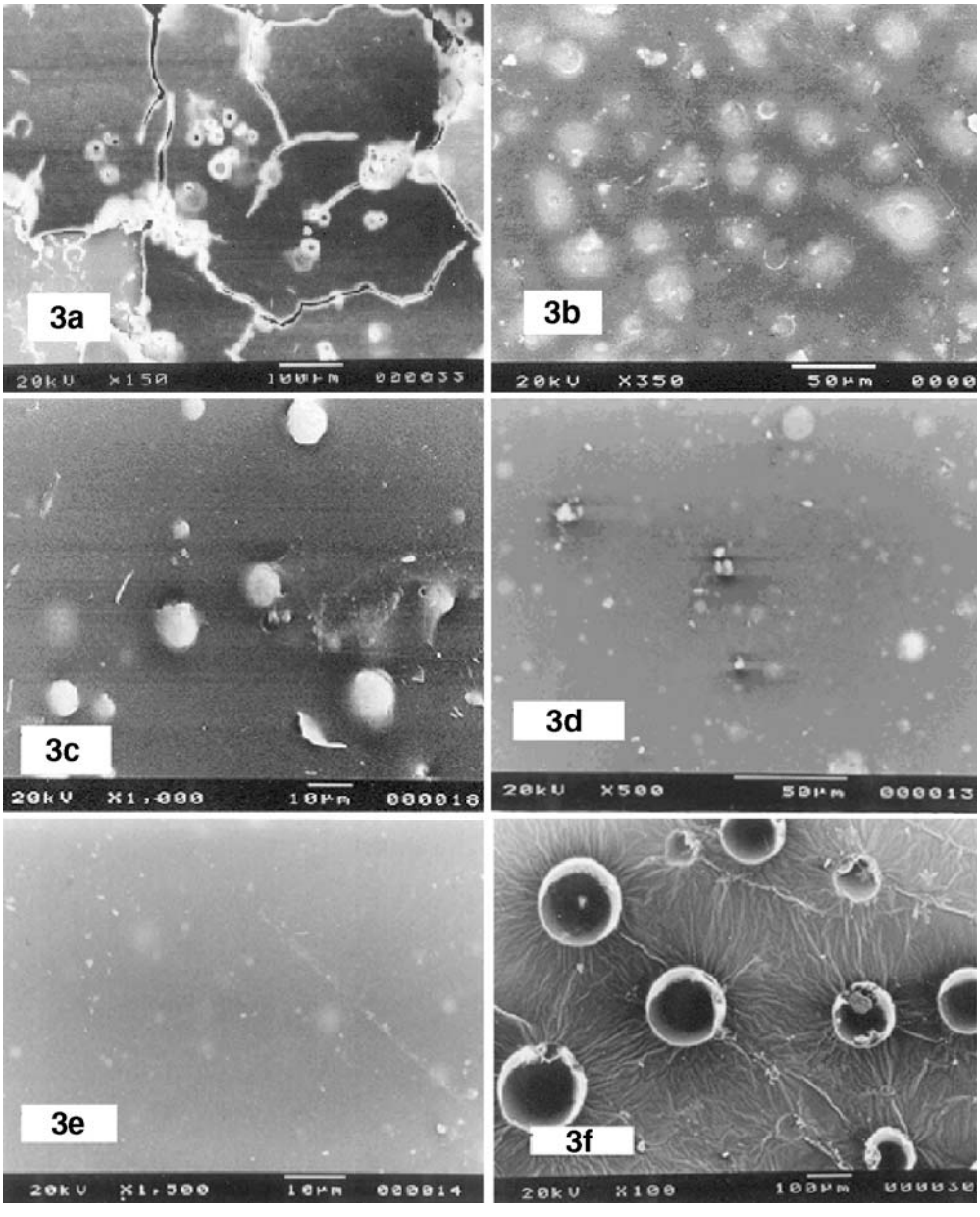

Fig. 3 **a** SEM micrograph for 0.028 PS:0.001 TEOS:0.0014 HCl:0.0793 Toluene. **b** SEM micrograph for 0.028 PS/MVS (1):0.0036 TEOS:0.007 HCl:0.0793 Toluene. **c** SEM micrograph for 3.19×10^{-3} PS/BA: 1.56×10^{-3} TEOS:2×10^{-4} HCl:0.123 THF. **d** SEM micrograph for PS/BA/MVS (1):4.34×10^{-3} TEOS:2×10^{-5} HCl:0.123 THF. **e** SEM micrograph for 2.86×10^{-3} PS/BA/MVS(2):6.5×10^{-3} TEOS:2.95×10^{-3} HCl:0.123 THF. **f** SEM micrograph for $2.86\times10{-3}$ PS/BA/MVS (2):8.9×10^{-3} TEOS:1.47×10^{-5} HCl:0.123 THF

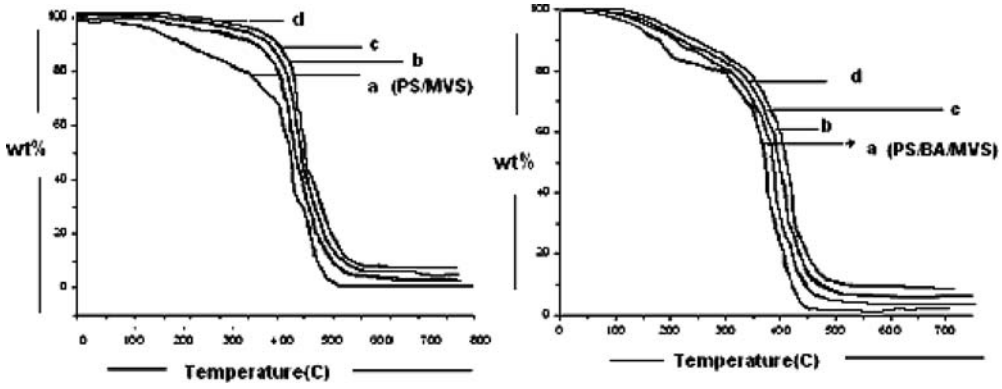

Fig. 4 **a** TGA curves for PS/MVS and its composites. **b** TGA curves for PS/BA/MVS and its composite

Conclusion

Comparison of (PS/MVS)/silica, (PS/BA)/silica, and (PS/BA/MVS)/silica sol–gel composites showed that optically transparent composites with the highest silica loading (~12.8%) were obtained for the composites derived with (PS/BA/MVS)/silica.That the addition of butyl acrylate enhanced compatibilization of silica with the polystyrene matrix was evident from SEM results which showed that the styrene–butyl acrylate copolymers could produce crack-free composites, whereas crack-free composites with polystyrene and silica could not be produced. TGA results showed enhancement of thermal stability in the hybrid composites, which may be attributed to interactions between the polymer chain and silica network. The thermal stability of the films was found to increase with an increase in the silane content in the copolymers and silica content in the composites. Among the four systems thermal stability and hydrophobicity was found to be highest for composites derived with silane functionalized polystyrene and silica [(PS/MVS)/silica]. The (PS/BA/MVS)/silica composites also show appreciable improvement in these properties as compared to the individual polymers due to the incorporation of a silica phase. These hybrid composites may find potential applications as sol–gel coatings, which can impart many useful properties to materials such as thermal, mechanical or chemical stability, wear protection, and durability.

Acknowledgement The authors gratefully acknowledge the Council of Scientific and Industrial Research (CSIR), Govt. of India for financial assistance in the form of a senior research fellowship to one of the authors.

References

1. Brinker CJ, Scherrer GW (1990) Sol–gel science: the physics and chemistry of sol–gel processing. Academic, San Diego
2. Hench LL, West JK (1990) Chem Rev 90:33
3. Cheetham K, Brinker CJ, Mc Cartney ML, Sanchez C (1994) Better ceramics through chemistry VI, vol 346. Materials Research Society, Pittsburg, PA
4. MJ Hampden-Smith, Klemperer WG, Brinker, CJ (ed) (1992) Better ceramics through chemistry V, vol 271. Materials Research Society, Pittsburg, PA
5. Corriu RJ, Leclercq D (1990) Angew Chem Int Ed Engl 35:1420
6. Zarzycki J (1997) J Sol–Gel Sci Technol 8:17
7. Sakka S (1992) Proc SPIE Int Soc Opt Eng 2:1758
8. Klonkiowski AM (1993) Wiad Chem 47:497
9. Mackenzie JD, Ulrich DR (1990) Proc SPIE Int Soc Opt Eng 2:1328
10. Laine RM (1990) Proc SPIE Int Soc Opt Eng 1328:16
11. Brinker, C Jeffrey (1994) SolGel Procesing of Silica. In: Bergna HE (ed) The colloid chemistry of silica advances in chemistry series. American Chemical Society, Washington DC, 234:359
12. Huang HH, Wilkes GL (1987) Polym Bull 18:455
13. Huang HH, Wilkes GL (1985) Polym Bull 14:557
14. Jiang CY, Mark JE (1984) Makromol Chem 185:2609
15. Mark JE, Sun C-C (1987) Polym Bull 18:259
16. Mauritz KA, Jones CK (1990) J Appl Polym Sci 40:1401
17. Kotoky Tapasi, Dolui SK (2004) J Sol–Gel Sci Technol 29:107–114
18. Kotoky Tapasi, Ray BC, Dolui SK (2003) J Polym Mater 20:257–265
19. Dyer JR (1965) Application of absorption Spectroscopy of organic compounds. Prentice Hall, Englewood Cliffs, NJ, USA, pp 33–35
20. Colthup Norman, Daly Lawrence H, Wiberly Stephen W. Introduction to infrared and raman spectroscopy. Academic Press, London, 342
21. Landry Christine JT, Coltrain K, Brady Brian K (1992) Polymer 33(7): 1486–1495
22. Yoldas BE (1989) J Non-Cryst Solids 110:38
23. Gev Hsu Ying, Jung Lin Fung (2000) J Appl Polym Sci 75:275–283